Electronic Supplementary Material (ESI) for Journal of Materials Chemistry A.

W supported on *g*-CN manifests high activity and selectivity for N_2 electroreduction to NH_3

Shuhua Wang, Wei Wei,* Xingshuai Lv, Baibiao Huang and Ying Dai*

School of Physics, State Key Laboratory of Crystal Materials, Shandong University, 250100 Jinan, China

* Corresponding authors:

weiw@sdu.edu.cn (W. Wei)

daiy60@sdu.edu.cn (Y. Dai)

Table S1 Structural parameters of *g*-CN and comparison with previous theoretical results: lattice constant (*a*), bond length of C–N ($d_{C–N}$) and C–C bonds ($d_{C–C}$), bond angle between two C–N bonds ($angle_{C\text{-}N\text{-}C}$) in the hexagonal holes.

	a (Å)	$d_{C–N}$ (Å)	$d_{C–C}$ (Å)	$angle_{C\text{-}N\text{-}C}$ (°)
g-CN	7.11	1.34	1.51	114.3
Ref.	7.13[1]	1.34[1]	1.51[1]	114.4[2]

Geometry coordinates (in Å) of *g*-CN (lattice constant: *a*=7.11 Å)

C	0.4388336666666675	0.8776673333333278	0.5000000000000000
C	0.1223326666666722	0.5611663333333325	0.5000000000000000
C	0.4388336666666675	0.5611663333333325	0.5000000000000000
C	0.5611663333333325	0.1223326666666722	0.5000000000000000
C	0.8776673333333278	0.4388336666666675	0.5000000000000000
C	0.5611663333333325	0.4388336666666675	0.5000000000000000
N	0.7784303749999992	0.5568607499999985	0.5000000000000000
N	0.4431392500000015	0.2215696250000008	0.5000000000000000
N	0.7784303749999992	0.2215696250000008	0.5000000000000000
N	0.2215696250000008	0.4431392500000015	0.5000000000000000
N	0.5568607499999985	0.7784303749999992	0.5000000000000000
N	0.2215696250000008	0.7784303749999992	0.5000000000000000

Table S2 Binding energy (E_b, eV) of TM atoms at the energetically most favorable sites and the charge transfer (ΔQ, e^-) after TM atoms anchored on *g*-CN with the lowest-energy configurations.

TM atom	Sc	Ti	V	Cr	Mn	Fe	Co	Ni	Cu	Zn	Mo	W
E_b(eV)	-7.86	-7.76	-6.57	-4.59	-3.76	-4.32	-4.57	-4.74	-3.26	-1.37	-5.46	-6.94
ΔQ	1.81	1.42	1.26	1.24	1.22	1.12	0.83	0.77	0.74	1.16	1.25	1.33

Table S3 Gibbs free energy change of N_2 adsorption (ΔG_{*N_2}) on W/*g*-CN with side-on and end-on configurations, and the Gibbs free energy change of *NNH (ΔG_{*NNH}) and $^*NH_3$ (ΔG_{*NH_3}) formation on surface of various TM/*g*-CN. The unit is eV.

TM atom	ΔG_{*N_2} (end-on)	ΔG_{*N_2} (side-on)	ΔG_{*NNH}	ΔG_{*NH_3}
Sc	-0.39	-0.10	1.18	0.07
Ti	-0.64	-0.25	0.81	-0.12
V	-0.31	0.16	0.86	-0.38
Cr	0.12	0.60		
Mn	0.03	0.35		
Fe	-0.42	0.15	1.02	-0.86
Co	-0.58	0.17	1.20	-1.00
Ni	-0.37		1.30	-1.17
Cu	-0.35		1.79	-1.47
Zn	-0.01			
Mo	-0.47	0.19	0.47	-0.09
W	-0.87	-0.19	0.34	0.19

Table S4 Gibbs free energy change of each elementary step for considered TM/*g*-CN (Ti, V, Mo, W) with N_2 end-on configuration. The unit is eV.

Reaction paths	Ti	V	Mo	W
$N_2 \rightarrow {}^*N_2$	-0.64	-0.30	-0.46	-0.87
${}^*N_2 \rightarrow {}^*NNH$	0.82	0.87	0.47	0.34
${}^*NNH \rightarrow {}^*NNH_2$	-0.35	-0.40	0.08	-0.17
${}^*NNH_2 \rightarrow {}^*N + NH_3$	0.24	-0.26	-0.96	-0.83
${}^*N \rightarrow {}^*NH$	-1.33	-0.78	-0.06	-0.33
${}^*NH \rightarrow {}^*NH_2$	-0.34	-0.30	-0.28	-0.04
${}^*NNH \rightarrow {}^*NHNH$	0.34	0.18	0.74	0.77
${}^*NHNH \rightarrow {}^*NHNH_2$	-0.50	-0.37	-0.50	-0.68
${}^*NHNH_2 \rightarrow {}^*NH_2NH_2$	0.13	-0.20	0.23	0.53
${}^*NH_2NH_2 \rightarrow {}^*NH_2 + NH_3$	-1.75	-1.36	-1.69	-1.99
${}^*NH_2 \rightarrow {}^*NH_3$	-0.11	-1.24	-0.10	0.19
${}^*NH_3 \rightarrow NH_3$	1.05	1.76	0.65	1.05

Table S5 Summary of the onset potential from available theoretical studies on N_2 electroreduction upon *g*-C_xN_y-based SACs. The unit is V.

Catalysts	B/ *g*-C_3N_4	Pt/ *g*-C_3N_4	W/ *g*-C_3N_4	Ti@NVs- *g*-C_3N_4	Ru@ C_3N_4	B/ *g*-C_2N	Mo/ *g*-C_2N	B/ *g*-CN
Onset potential	0.20[3]	0.24[4]	0.31[5]	0.51[6]	0.33[7]	0.15[8]	0.17[9]	0.31[10]

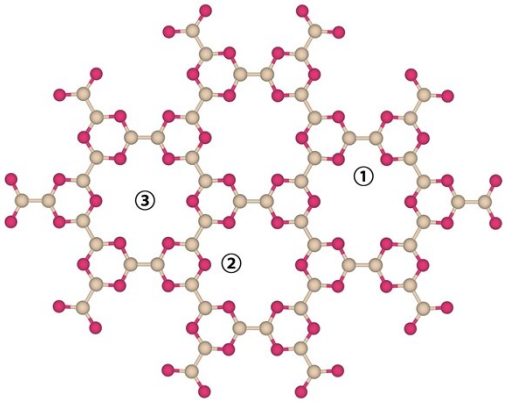

Figure S1 Three possible sites for TM atoms adsorption on *g*-CN.

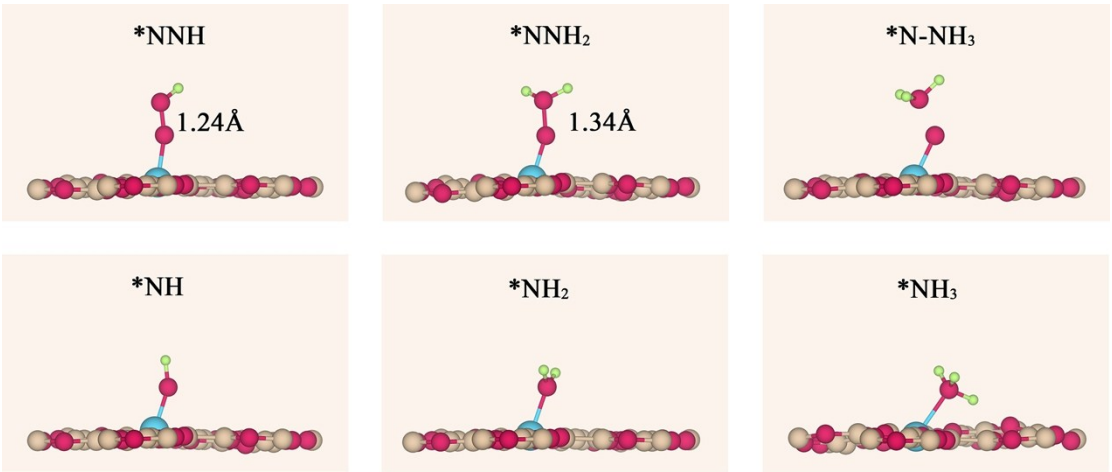

Figure S2 Optimized strcutures of various reduction intermediates on W/*g*-CN through the distal pathway. N–N bond lengths are highlighted.

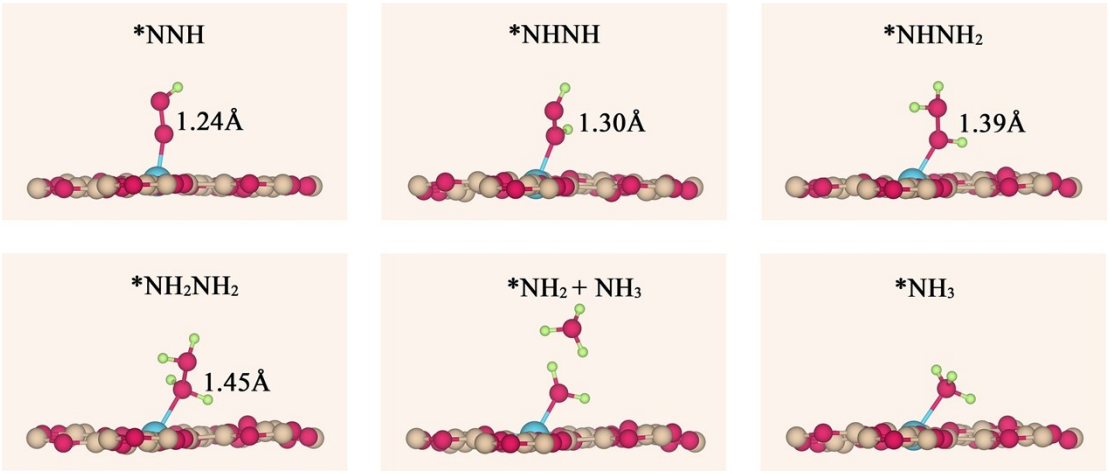

Figure S3 Optimized strcutures of various reduction intermediates on W/*g*-CN through the alternating pathway. N–N bond lengths are highlighted.

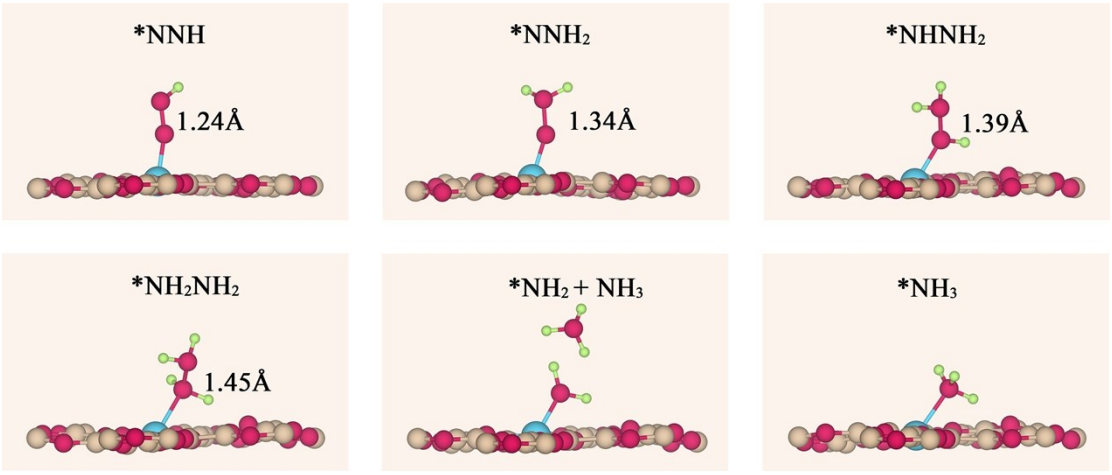

Figure S4 Optimized strcutures of various reduction intermediates on W/*g*-CN through the mixed pathway. N–N bond lengths are highlighted.

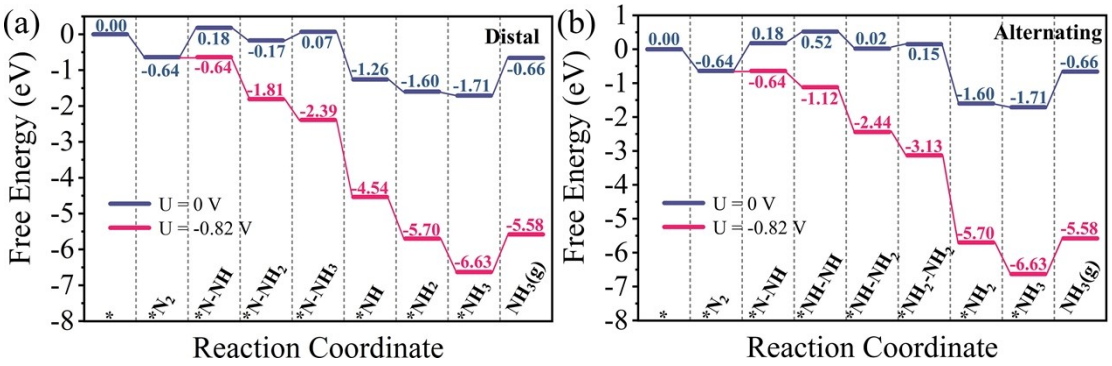

Figure S5 Gibbs free energy diagrams and the reduction intermediates for NRR on Ti/*g*-CN along different pathways.

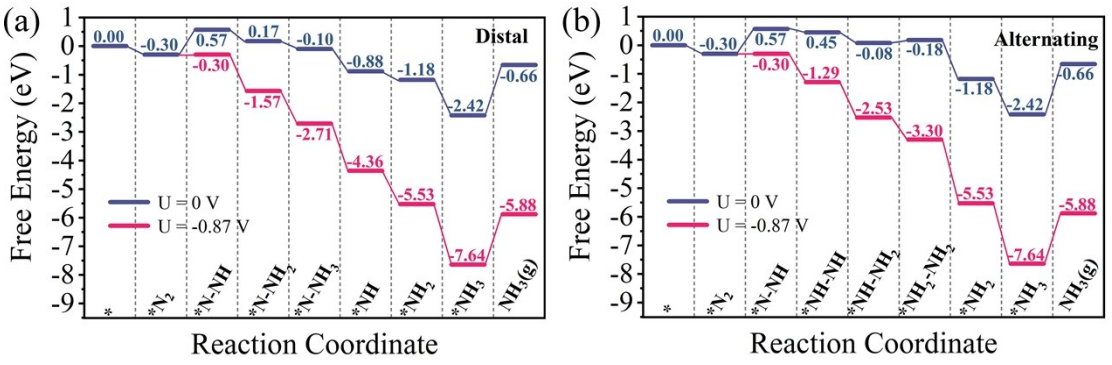

Figure S6 Gibbs free energy diagrams and the reduction intermediates for NRR on V/*g*-CN along different pathways.

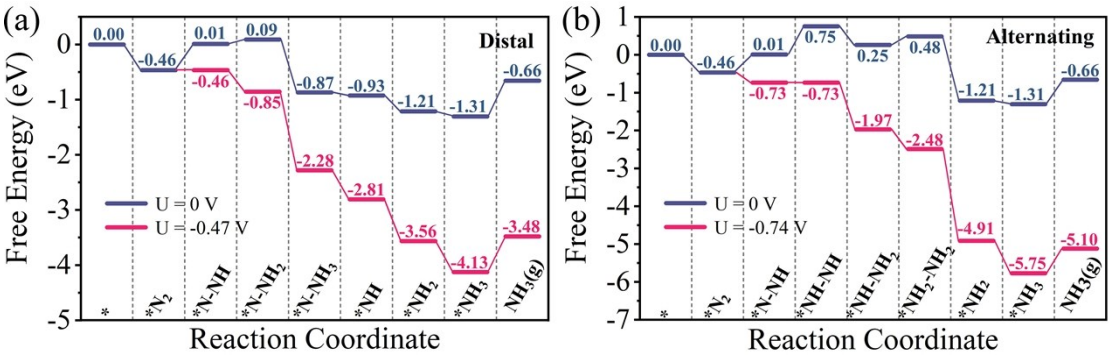

Figure S7 Gibbs free energy diagrams and the reduction intermediates for NRR on Mo/*g*-CN along different pathways.

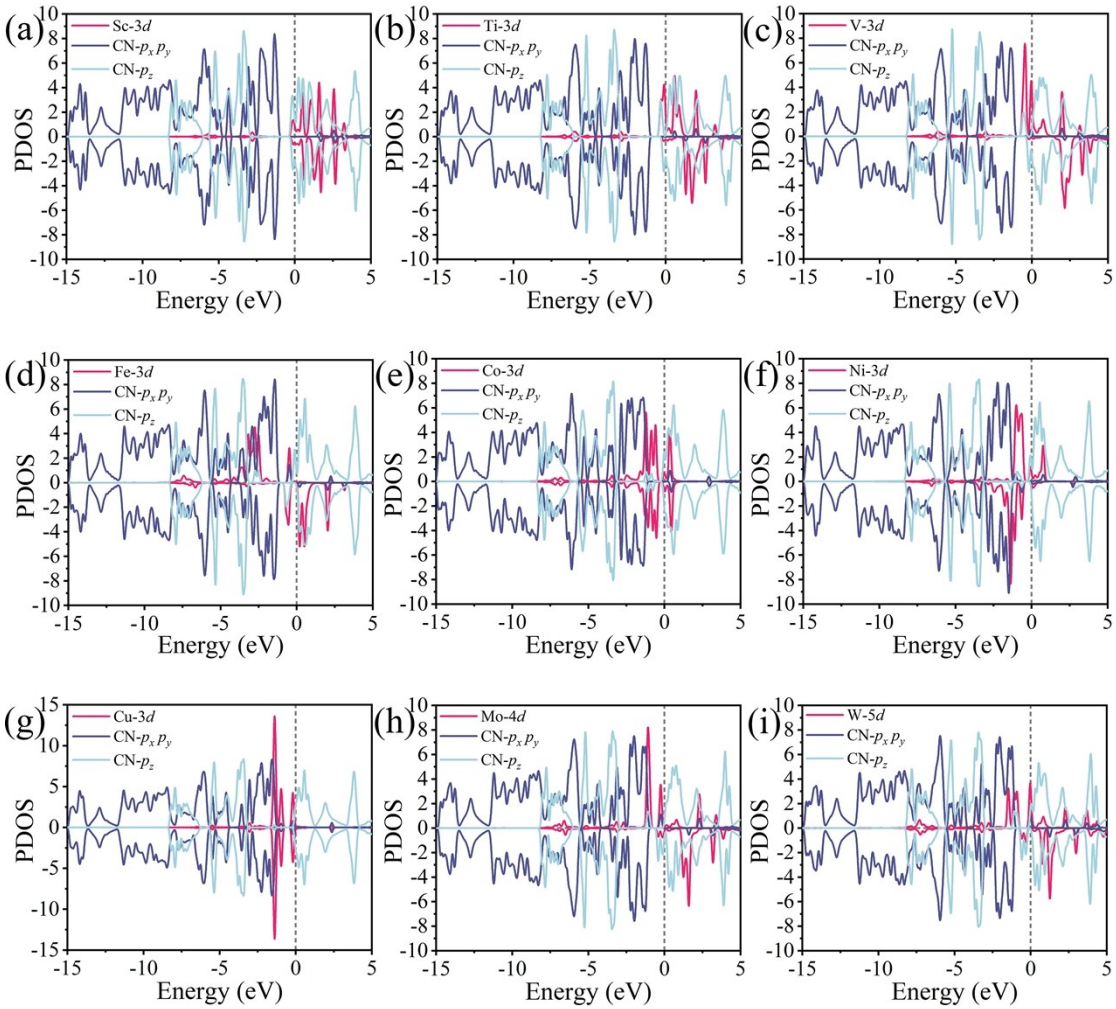

Figure S8 (a)–(i) Projected density of states (PDOS) of TM and *g*-CN before N_2 adsorption.

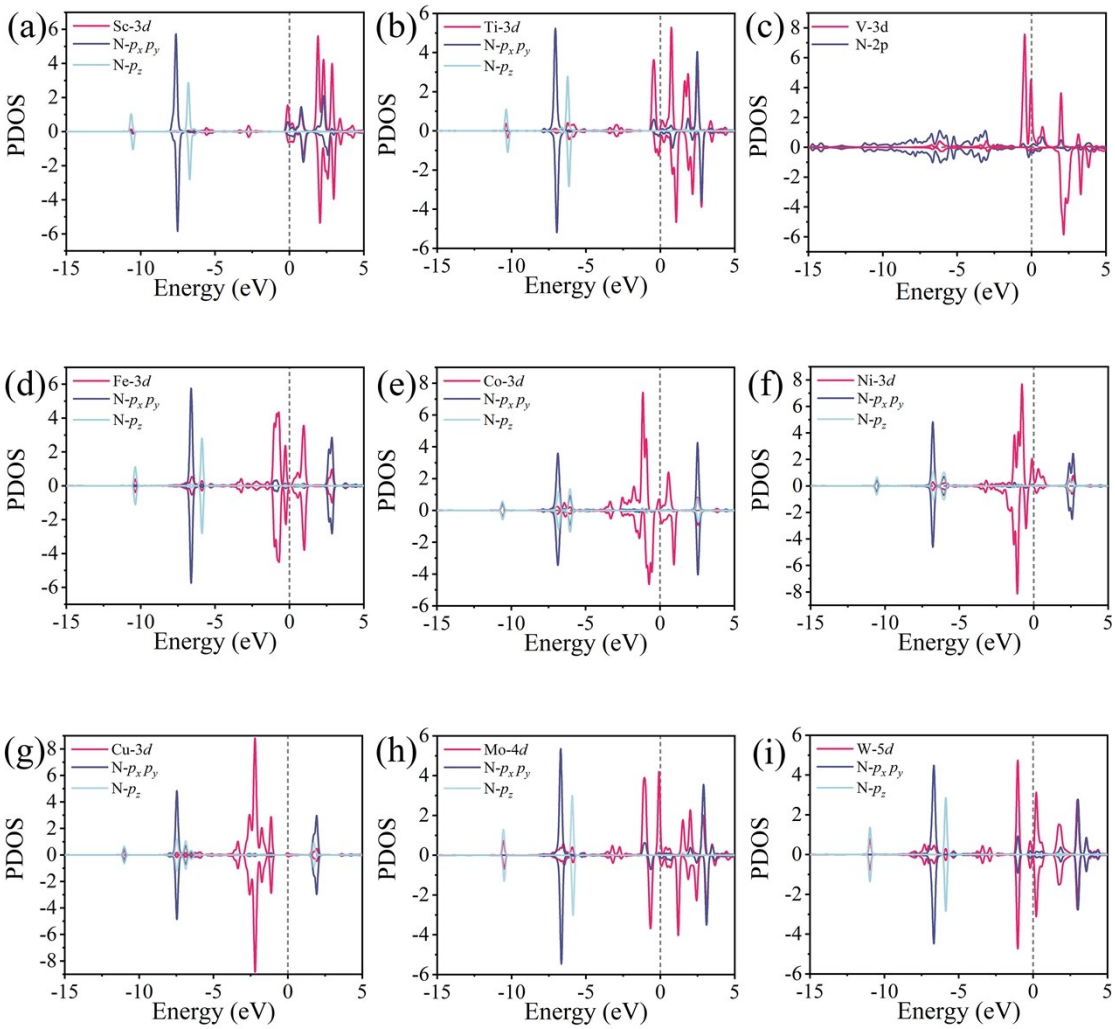

Figure S9 (a)–(i) Projected density of states (PDOS) of TM and N_2 after N_2 adsorption.

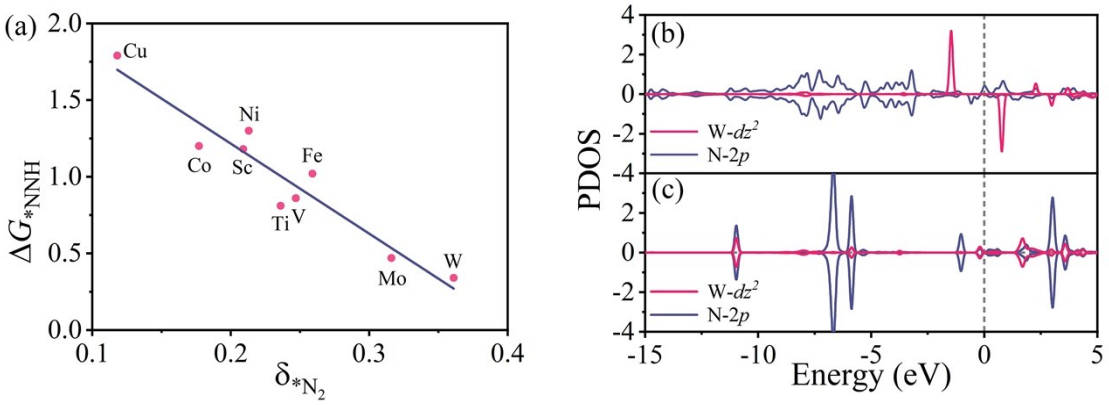

Figure S10 (a) Free energy change of *NNH formation as a function of the quantity of transferred electrons on N_2. Projected density of states (PDOS) of (b) W (d_{z^2}) and adjcent N (2p) before N_2 adsorption on W/g-CN, and (c) W (d_{z^2}) and N_2 (2p) after N_2 adsorption.

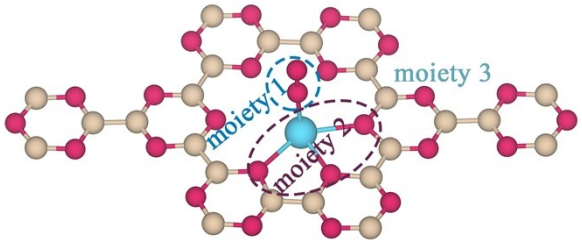

Figure S11 Schematic for the partition of the three moieties on W/g-CN with N_xH_y adsorption.

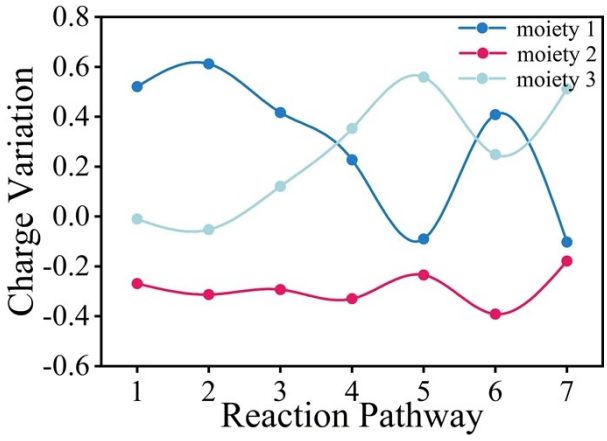

Figure S12 Charge variation of three moieties for NRR over W/*g*-CN along the alternating pathway.

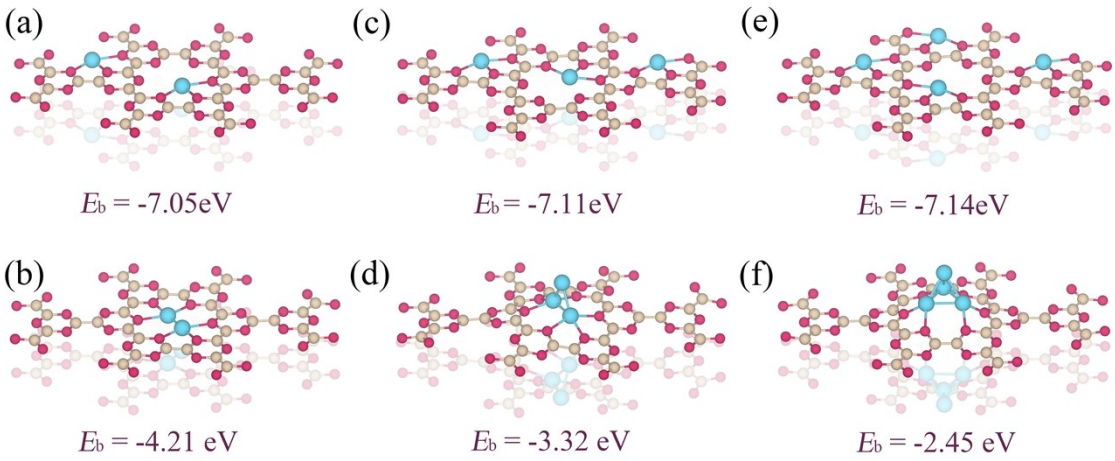

Figure S13 Structures and binding energies per W atom on *g*-CN with the adsorption of (a) two W single atoms, (b) W_2 cluster, (c) three W single atoms, (d) W_3 cluster, (e) four W single atoms and (f) W_4 cluster.

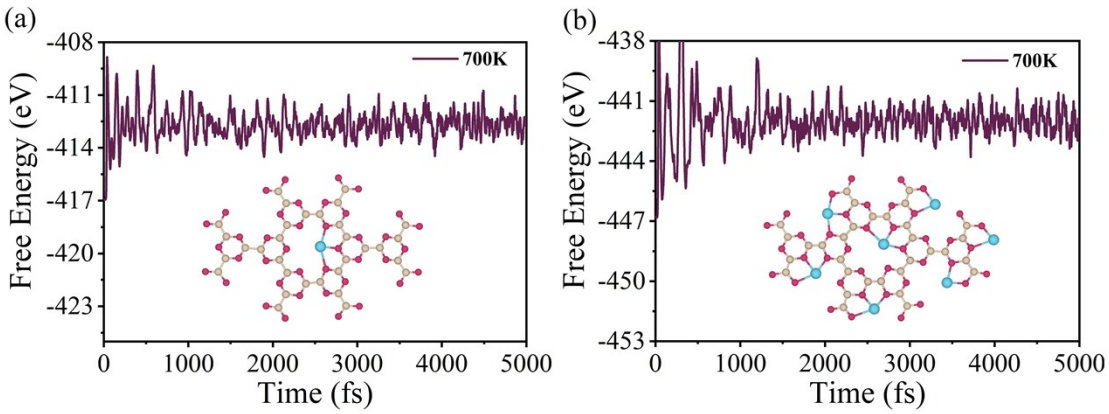

Figure S14 Free energy variation versus AIMD simulation for *g*-CN with (a) 25% (one atom per 2×2×1 cell) and (b) 100% (four atoms per 2×2×1 cell) W loading concentrations. Insets show the structure of W/*g*-CN after AIMD simulation after 5 ps at T = 700 K.

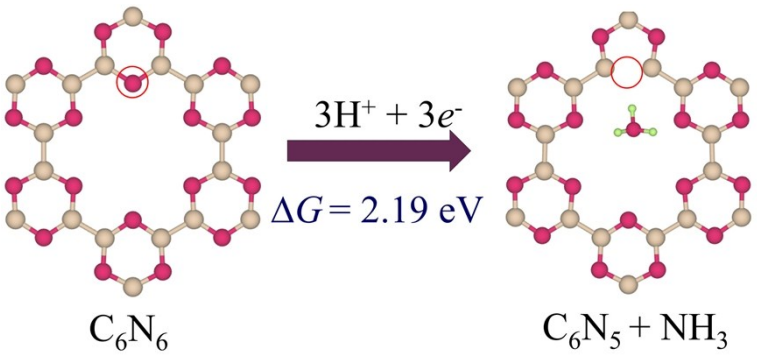

Figure S15 Schematic of the decomposition of nitrogenous substrate by protonation., with the free energy change in the process denoted.

Note 1

The decomposition of *g*-CN substrate to release NH_3 can be expressed as:

$$C_6N_6 + 3H^+ + 3e^- \rightarrow C_6N_5 + NH_3\,(g)$$

where C_6N_6 represents *g*-CN substrate, and C_6N_5 represents the remaining structure after losing one nitrogen atom.

The overall free energy change for the decomposition reaction can be expressed following:

$$\Delta E_d = E_{C_6N_5} + E_{NH_3} - E_{C_6N_6} - 3E_{H^+ + e^-}$$

$$\Delta G_d = \Delta E_d + \Delta E_{ZPE} - T\Delta S$$

Here $E_{C_6N_5}$, E_{NH_3}, $E_{C_6N_6}$ and $E_{H^+ + e^-}$ represent the energy of remaining structure after decomposition, ammonia molecule, *g*-CN substrate and proton/electron pair, respectively. Hence the required decomposition potential can be expressed as:

$$U_d = -\Delta G_d/3e$$

References

1 K. Srinivasu, B. Modak and S. Ghosh, *J. Phys. Chem. C*, 2014, **118**, 26479–26484.

2 A. Wang, X. Zhang and M. Zhao, *Nanoscale*, 2014, **6**, 11157–11162.

3 C. Ling, X. Niu, Q. Li, A. Du and J. Wang, *J. Am. Chem. Soc.*, 2018, **140**, 14161–14168.

4 H. Yin, S. Li, L. Gan and P. Wang, *J. Mater. Chem. A*, 2019, **7**, 11908–11914.

5 Z. Chen, J. Zhao, C. R. Cabrera and Z. Chen, *Small Methods*, 2018, **3**, 1800368.

6 X. Chen, X. Zhao, Z. Kong, W. Ong and N. Li, *J. Mater. Chem. A*, 2018, **6**, 21941–21948.

7 X. Liu, Y. Jiao, Y. Zheng, M. Jaroniec and S.-Z. Qiao, *J. Am. Chem. Soc.*, 2019, **141**, 9664–9672.

8 S. Ji, Z. Wang and J. Zhao, *J. Mater. Chem. A*, 2019, **7**, 2392–2399.

9 Z. Wang, Z. Yu and J. Zhao, *Phys. Chem. Chem. Phys.*, 2018, **20**, 12835–12844.

10 X. Lv, W. Wei. F. Li, B. Huang and Y. Dai, *Nano Lett.*, 2019, **19**, 6391–6399.